International Journal of Fluid Machinery and Systems
Vol. 9, No. 3, July-September 2016
DOI: http://dx.doi.org/10.5293/IJFMS.2016.9.3.237
ISSN (Online): 1882-9554

Original Paper

Analysis on Characteristic of Pressure Fluctuation in Hydraulic Turbine with Guide Vane

FengXia Shi , JunHu Yang and XiaoHui Wang

School of Energy and Power Engineering, Lanzhou University of Technology
Lanzhou, 730050, China, shifengxia_168@126.com, lzyangjh@lut.cn

Abstract

An unsteady three-dimensional simulation based on Reynolds time-averaged governing equation and RNG *k*-ε turbulence model, was presented for pump-as-turbine, the pressure fluctuation characteristic of hydraulic turbine with guide vane was obtained. The results show that the time domains of pressure fluctuation in volute change periodically and have identical cycles. In volute tongue and inlet pressure fluctuations are light, while in dynamic and static coupling interface pressure fluctuations are serious; In impeller blade region the pressure fluctuation of pressure surface are lighter than that of suction surface. The dominant frequencies of pressure fluctuation concentrate in low frequency region, and concentrate within 2 times of the blade passing frequency.

Keywords: Hydraulic turbine with guide vane, Volute tongue, Dynamic and static coupling interface, Pressure fluctuation

1. Introduction

In general pump-as-turbine is used to recover residual pressure energy of high pressure fluid, and has a high efficiency, so it is applied widely in petrochemical engineering、desalination plant and ferrous metallurgy[1-6], etc. But this kind of hydraulic turbine belongs to typical rotary machinery, the operating condition of which is very narrow, and vibration always appears. There are three types of vibrations for hydraulic turbine: mechanical vibration、electromagnetic vibration and hydraulic vibration. Mechanical vibration is caused by the mechanical design and manufacturing, while electromagnetic vibration is caused by the vibration of motor, currently these two vibrations had been perfectly solved through active control technology[7-8]; Hydraulic vibration is mainly caused by pressure fluctuation in hydraulic turbine, and pressure fluctuation is one of the key factors of affecting the stability of turbine unit , so it is important to analyse the pressure fluctuation for the solution of hydraulic vibration. Several research studies have indicated that the efficiency can be improved and the radial force can be reduced by adding guide vane[9] , but the hydraulic vibration still exists, so the pressure fluctuation for hydraulic turbine with guide vane needs to be studied to further understand the vibration problem. The research for the pressure fluctuation of hydraulic turbine with guide vane is scarce, but the experiences of pressure fluctuation in centrifugal pumps and other hydraulic machineries can be used for reference. A lot of research studies about pressure fluctuation for centrifugal pump and hydraulic turbine have been done by researchers. Experiments [10-13]and numerical calculations[14-15] are the main method. In this paper, the hydraulic turbine with guide vane in a chemical plant in operation is studied, an unsteady three-dimensional simulation based on Reynolds time-averaged governing equations and RNG k-ε turbulence model is presented for hydraulic turbine with guide vane, the pressure fluctuation characteristic of which is obtained, and the theoretical basis for the stability of hydraulic turbine operation is provided.

2. Calculation model and monitoring position

Different from other hydraulic turbines, in this paper the hydraulic turbine model consists of three parts: volute、guide vane and impeller. Under the design condition, the flow rate $Q = 63m^3/h$, the head $H = 81m$, the speed $n = 2980r/\min$. The performance parameter of turbine is shown in table 1. Figure 1 shows the position of points. There are totally 9 points (P1、P2、P3、P4、P5、S1、 D1、P6、P7): P1 is near the volute tongue, P2、P3、P4 and P5 are in the dynamic and static coupling interface, S1 is selected in the inlet of turbine, D1 is near the impeller outlet; In addition, P6、P7 are respectively in suction side and pressure side of the impeller.

Received July 10 2015; revised November 26 2015; accepted for publication January 8 2016: Review conducted by Zhongdong Qian
(Paper number O15033C)
Corresponding author: Jun Hu Yang, Professor, lzyangjh@lut.cn

Table 1 main geometric parameters of hydraulic turbine

Impeller						Guide vane				
D_2	D_1	B_2	Z_1	β_2	β_1	S	Z_2	L	β_3	β_4
276	90	6	5	38	30	4	6	30	9	13

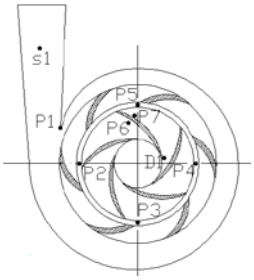

Fig.1 Monitoring points in the hydraulic turbine with guide vanes

3.Numerical method

Currently both large eddy simulation and Reynolds time-averaged are adopted to deal with the problem of pressure fluctuation for centrifugal pumps. By contrast, Reynolds time-averaged method has a low requirement on grid, computer and calculation time[16-17], so in this paper Reynolds time-averaged and RNG $k-\varepsilon$ model are adopted, the unstructured grids are meshed, and the grid independence is verified under steady state, the relation curve of grid number and efficiency is shown in Fig. 2, firstly the efficiency increases rapidly with the grid number increases, and then increases slowly, when the grid number increases to 900000, the change range of efficiency is less than 0.5%, so the grid number more than 900000 is more appropriate, the final grid number is 1042502. The grids in computational region is shown in Fig. 3.

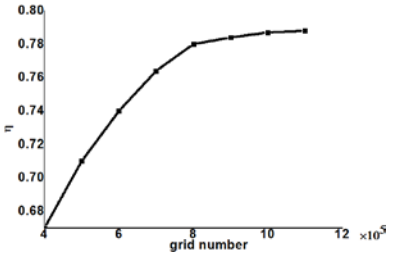

Fig.2 relation curve of grid number and efficiency

Fig.3 Grids in computational region

In the process of unsteady numerical simulation, sliding mesh technology is performed inside the static and dynamic coupling interface of hydraulic turbine with guide vane, PISO algorithm is adopted for the simultaneous solution of the momentum equation and continuity equation. Velocity condition is used for the inlet boundary condition, pressure condition is used for the outlet boundary condition. Solid walls of hydraulic model include volute and guide vane, in which no slip boundary condition is adopted. The calculation accuracy of convergence is 10^{-4}, a complete calculation is done from inlet of volute to outlet of impeller. The unsteady calculation is based on the steady calculation convergence. The time step of unsteady numerical simulation is 2.013×10^{-4}s, and the angle of rotation of the impeller for each cycle is 360°, so every 100 time steps the impeller rotates one circle. The impeller totally rotated five cycles during the process of unsteady calculation, and the data of the fifth circle is adopted for analysis. The rotation speed of the hydraulic turbine is n=2980r / min, and the vane numbers of impeller is Z= 5, so the frequency of rotation is f=49.67Hz, and the blade passing frequency (product of the rotation frequency and blade numbers) is f=248.35Hz.

4.Test

The test bench for hydraulic turbine is shown in Fig. 4. The accuracy of the numerical calculation is verified by experiment.

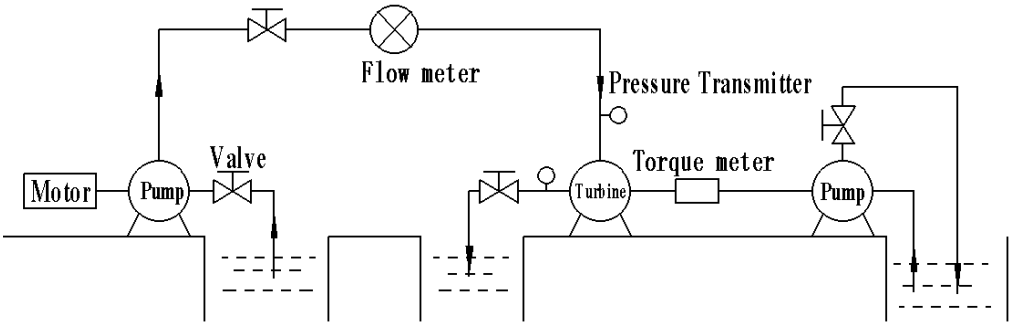

Fig.4 Test bench for hydraulic turbine

Figure 5 lists the comparison between experimental and numerical performance curves. As is shown in Fig. 5, the tendency of hydraulic turbine's numerical predicted performance curves agree well with that of experimental. Numerical predicted efficiency and head are higher than those of experimental, the reason is that in numerical calculation the leakage loss through balancing holes and mechanical loss caused by mechanical seal and bearings are not included. At the best efficiency point the relative error of efficiency and head is 4.82% and 3.6% respectively, it is fully proved that RNG k-ε turbulence model in the description of fully developed turbulent flow has good applicability, so the numerical method can better predicts the performance of the hydraulic turbine, can be used to calculates the pressure fluctuation of hydraulic turbine.

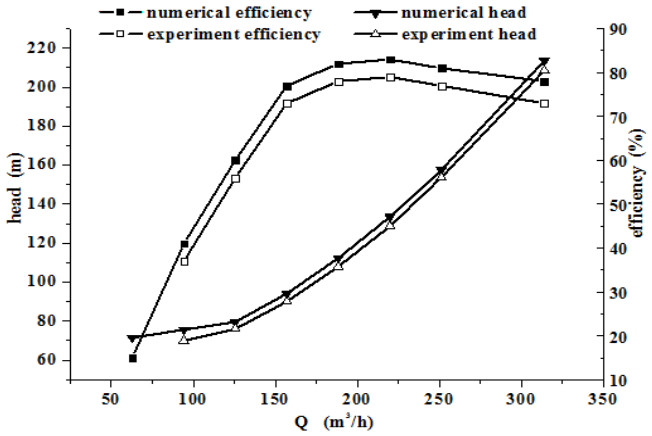

Fig.5 Comparison between experimental and numerical performance curves

5. Results and analysis

5.1 Static pressure contour inside hydraulic turbine with guide vane

Take one impeller blade as a mark, and according to the blade passes through different position, a cycle(T)is divided into five moments: $t=\frac{1}{5}T$, $t=\frac{2}{5}T$, $t=\frac{3}{5}T$, $t=\frac{4}{5}T$ and $t=\frac{5}{5}T$, the static pressure contour in volute and guide vane at different moment is shown in Fig.6. At different moment the internal pressure of hydraulic turbine with guide vane changes obviously, and reduces gradually from inlet to outlet. Assuming that $t=\frac{1}{5}T$ is the initial moment, so at the $t=\frac{2}{5}T$ moment the impeller blade passes the volute tongue, where the static pressure increases obviously and distributed uneven, even more, an obvious high pressure area appears, the reason is that when the liquid impacts volute tongue the velocity of liquid reduced,which leads the liquid gathered and a high presure area appeared around volute tongue. After the impeller blade goes away from volute tongue, the static presure distribution gradually becomes even, and the presure distributes more even at $t=\frac{3}{5}T$ and $t=\frac{4}{5}T$. The hydraulic turbine with guide vane has rotated one circle at $t=\frac{5}{5}T$, and returns to the initial position.

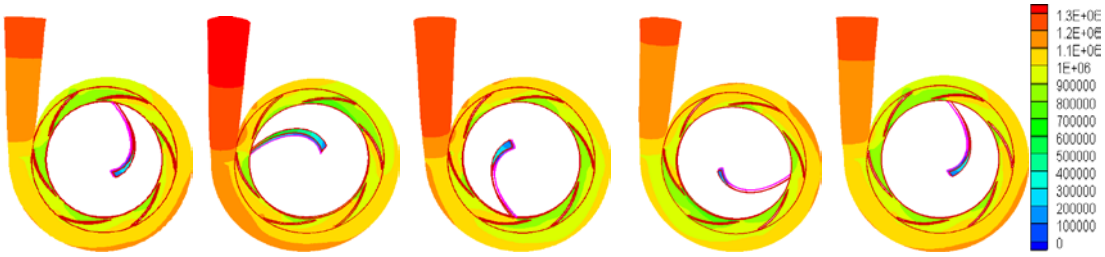

$t=\frac{1}{5}T$ $t=\frac{2}{5}T$ $t=\frac{3}{5}T$ $t=\frac{4}{5}T$ $t=\frac{5}{5}T$

Fig.6 Static pressure contour in volute and guide vane at the different moment

5.2 Pressure fluctuation characteristics in inlet and outlet of the hydraulic turbine with guide vane

The time domain spectrums of monitoring points S1、D1 are shown respectively in Fig. 7 and Fig. 8. The abscissa represents time in one cycle(the fifth rotating cycle is 0.082~0.10s), the ordinate represents static pressures. Totally four conditions are

simulated:0.8Qe、Qe、1.2Qe and 1.4Qe, Qe is the flow rate of the best efficiency point.

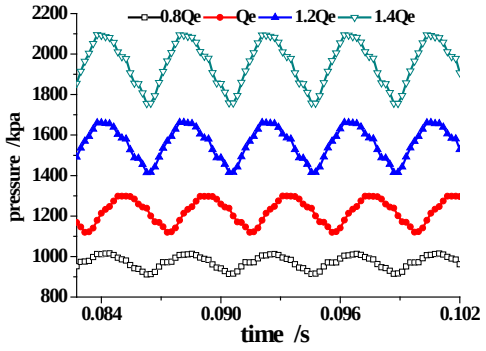

Fig.7 Time-domain spectrums of monitor point S1

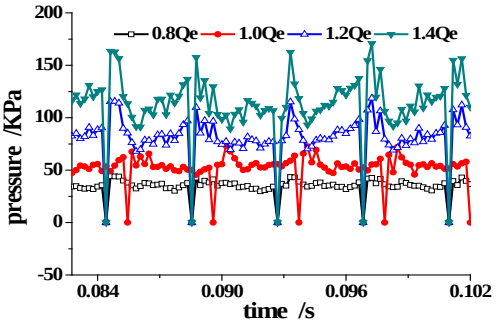

Fig.8 Time-domain spectrums of monitoring point D1

The static pressure differences of monitor points S1、D1 are shown in Table 2, and the static pressure differences is defined as $P^{'}$:

$$P^{'} = P - \Delta P \tag{1}$$

P — the maximum instantaneous static pressure;

ΔP —the average static pressure.

Table 2 The static pressure differences of monitoring points S1、D1 (kpa)

Flow rate (Q/Qe)		0.8	1.0	1.2	1.4
pressure	S1	45.03	76	106.90	148.42
	D1	9.8	20.5	37.8	58.65

From Fig. 7 and Table 2: the pressure fluctuation in inlet of turbine is periodical, and becomes greater with the flow rate increases. In 0.8Qe condition, the inlet pressure and pressure fluctuation are the smallest; Contrary in 1.4Qe condition, the inlet pressure and corresponding pressure fluctuation are the biggest. From Table 2 and Fig.8: the pressure fluctuation in outlet increases with the flow rate increases, the static pressure difference in optimal condition is 20.5Kpa. the pressure fluctuations is relatively disordered in each fluctuation cycle, and tiny wave is found. The greater the flow rate, the more serious of the tiny wave, the reason is that from inlet to outlet most of the pressure energy of liquid had been consumed, and in impeller outlet liquid pressure greatly reduced, the liquid casted off the constraint of impeller. Compared with the value of inlet(45.03～148.42kpa), the static pressure difference in outlet reduced greatly, which only is 9.8～58.65kpa.

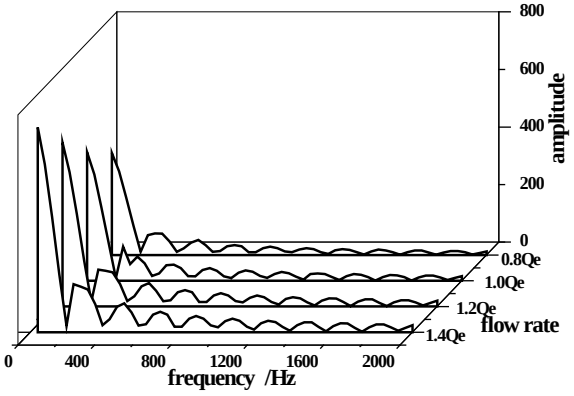

Fig.9 Frequency spectrums of monitoring point S1

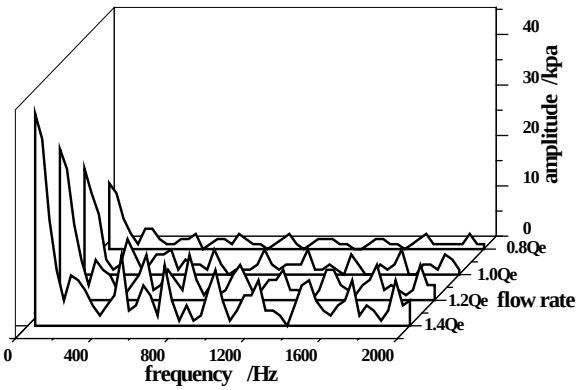

Fig.10 Frequency spectrums of monitoring point D1

Figure 9 shows the corresponding frequency spectrums of S1, which is transformed from Fig.7 through FFT（Fast Fourier Transform）. The abscissa represents frequency, the ordinate represents amplitude of pressure fluctuation. From Fig 9: the main fluctuation frequencies of S1 are less than 40Hz, which is less than the frequency of rotation (f=49.67Hz). With different flow rate, the pressure fluctuation amplitude is also different. The fluctuation amplitude in 1.0Qe condition is 447kpa, which is 1.25 times of amplitude in 0.8Qe condition; The fluctuation amplitude in 1.4Qe condition is 712kpa, which is 1.6 times of amplitude in1.0Qe condition, but all the main frequencies of different conditions are identical.

The frequency spectrums of monitoring point D1 are shown in Fig.10. The main frequency of pressure fluctuation concentrates in low frequency region, in high frequency region which is smaller, and has little effects on the flow state of outlet. All the frequencies of pressure fluctuation are less than rotating frequency.

5.3 Pressure fluctuation characteristics of volute tongue, dynamic and static coupling interface

The static pressure differences of P1～P5 in volute tongue and static and dynamic coupling interface are shown in table 3. The time-domain spectrums of P1～P5 under optimal condition are shown in Fig. 11.

Table 3 The static pressure differences of P1～P5 at the best efficiency (kpa)

Flow ratio (Q/Qe)		0.8	1.0	1.2	1.4
pressure	P1	48	77	101	137
	P2	49	82	109	153
	P3	101	238	339	440
	P4	48	67	93	120
	P5	103	193	293	389

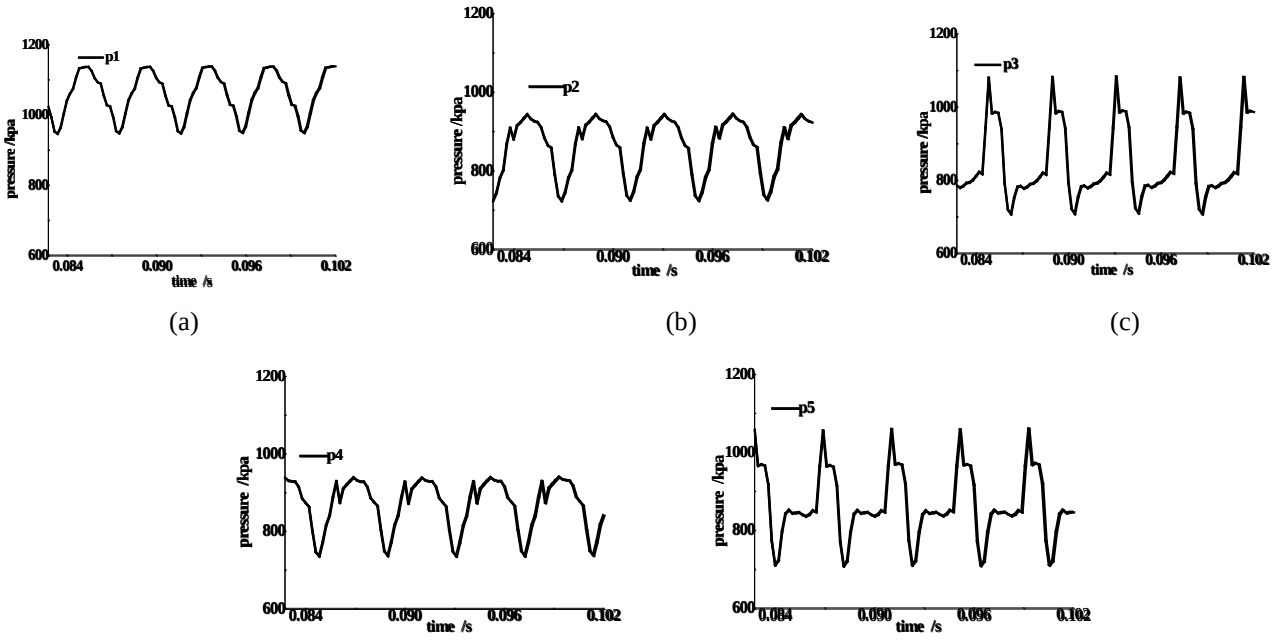

(a) (b) (c)

(d) (e)

Fig.11 Time-domain spectrums of P1～P5 at the best efficiency

(a) P1 (b) P2 (c) P3 (d) P4 (e)P5

From table 3 and Fig. 11: the pressure fluctuation of each point is a periodic variation, and with a same cycle. P1 locates the volute tongue, which is near the inlet, so the flow loss is the minimum, the static pressure is the maximum, and after FFT the amplitude of pressure fluctuation is also the maximum, but the pressure fluctuation amplitude difference is lesser, so in volute tongue the pressure fluctuation is minor, this result is in accord with reference [14]. The static pressure difference P1 is 7.2 percent of the average static pressure. Points P2～P5 are in the dynamic and static coupling interface, the static pressure difference of P2 and P4 are smaller, but P3 and P5 are biggish. Among four points, the static pressure difference of P4 is the minimum, which is 7.6 percent of the average static pressure, the static pressure difference of P3 is the maximum, which is 28.2 percent of the average static pressure. In addition, during the process of pressure fluctuation changes with time, the pressure fluctuation waveform of P2 and P4 are alike, P3 and P5 are alike, while they are just half cycle apart respectively.

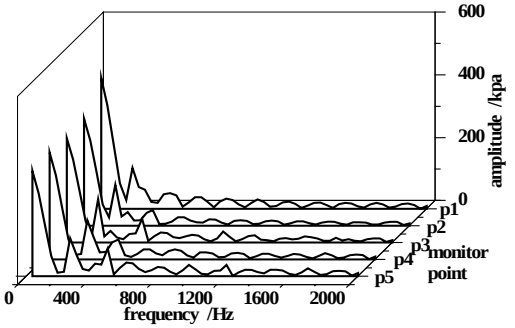

Fig.12 Frequency spectrums of monitoring points P1～P5 at the best efficiency

The frequency spectrums of monitoring points P1～P5 are shown in Fig. 12. Major pressure fluctuation amplitudes are concentrated in low frequency region, the main frequencies of each point are mainly low frequency. There are two obvious frequencies within 400Hz: the first one is near the 1 time rotation frequency, the second is near the 1 time blade passing frequency.

the frequencies of outside 400Hz have little effects on the pressure fluctuation, so the pressure fluctuations in dynamic and static interference are mainly to low rotating frequencies and blade passing frequencies.

4.4 Pressure fluctuation characteristics in blade region

Table 4 The static pressure differences of monitoring points P6、P7(kpa)

Flow ratio (Q/Qe)		0.8	1.0	1.2	1.4
pressure	P6	124.7	167.67	229.04	342.04
	P7	76.08	131.69	189.40	285.52

The static pressure differences of monitor points P6、P7 in blade region are shown in Table 4. The static pressure difference increases with the flow rate increases. For the same flow rate, the amplitude difference of P6 is greater than that of P7, and at the best efficiency the static pressure difference of P6 is 1.27 times of P7.

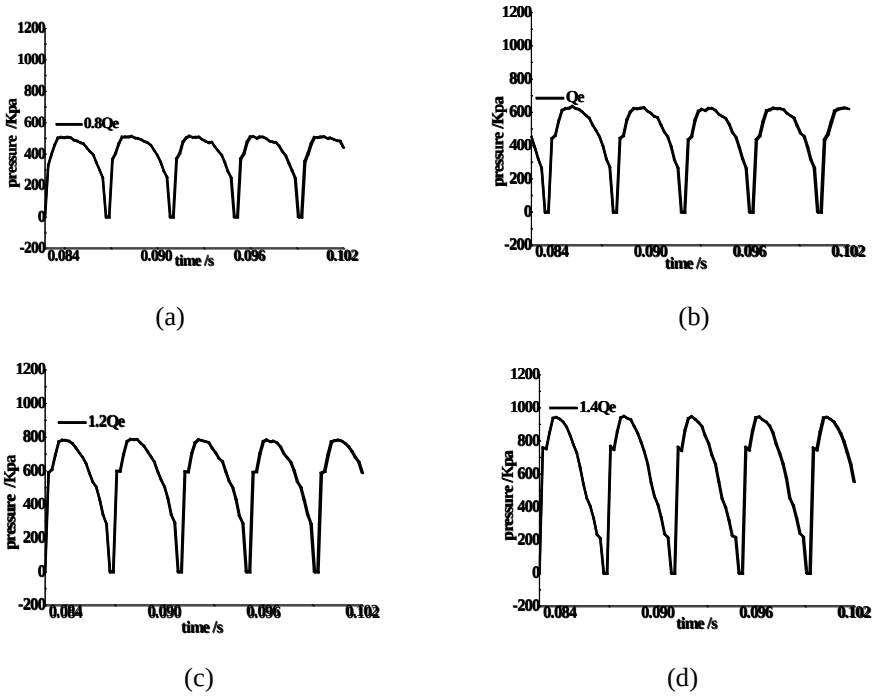

Fig.13 Time-domain spectrums of monitoring point P6 in different operating conditions

Figure 13 and Fig. 14 respectively shows the time-domain spectrums and frequency spectrums of monitor points P6. The time-domain spectrum of P6 is a sinusoidal variation, and two complete fluctuation periods are included in one rotation cycle, the greater the flow rate, the greater the amplitude of pressure fluctuation. In 0.8Qe and Qe conditions, the maximum pressure amplitudes appear near the 1 time of rotation frequency, while in 1.2Qe and 1.4Qe conditions which occur in the vicinity of the 1 time of blade passing frequency, so for small flow rate the pressure fluctuation frequencies are mainly to rotation frequecies, for large flow rate the rotating frequencies and blade passing frequencies exist simultaneously.

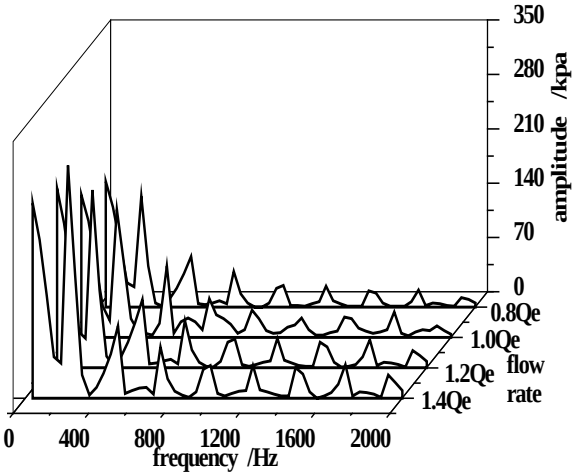

Fig.14 Frequency spectrums of monitoring point P6

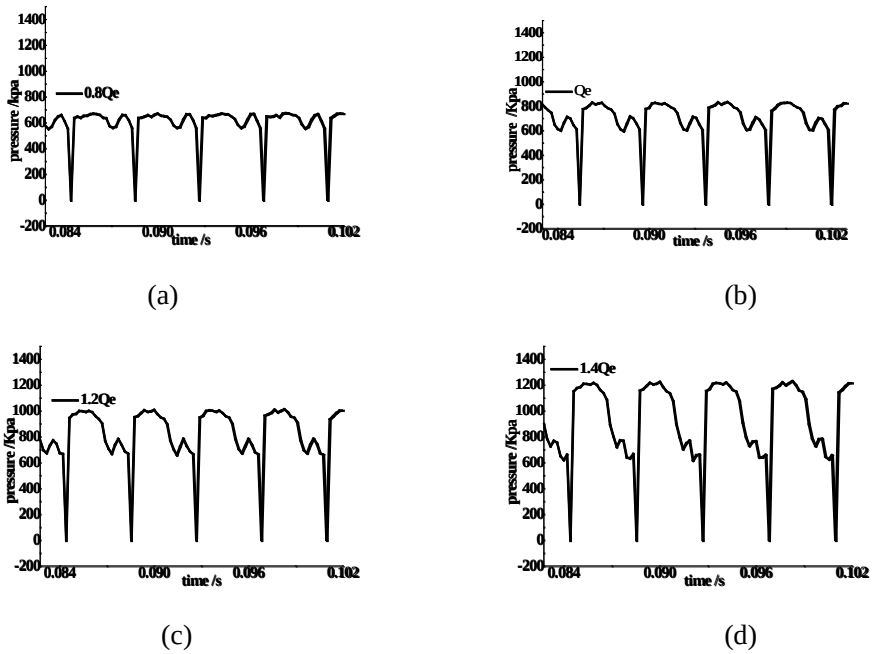

Fig.15. Time-domain spectrums of monitoring point P7 in different operating conditions

The time-domain spectrums and frequency spectrums of P7 are shown in Fig.15 and Fig.16. Time domain presents a periodic change, two times pressure fluctuation appears in each fluctuation cycle, the greater the flow rate, the more obvious the two times fluctuation, and the greater the amplitude difference of pressure fluctuation. The static pressure difference in 1.4Qe is 3.75 times of that in 0.8Qe. From Fig.16: the main frequencies of pressure fluctuation appear in the low frequency region, the amplitude of main frequency increases with the flow rate increases. In different conditions the main frequencies are identical and near the 1 time rotating frequency.

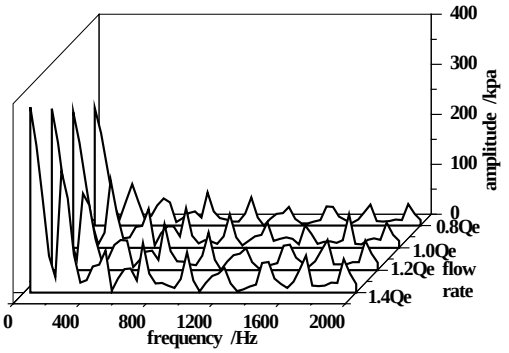

Fig.16 Frequency spectrums of monitoring point P7

5. Conclusions

To hydraulic turbine with guide vane, because of its special technics, operating condition is narrow, so the pressure fluctuation exists in any condition, and changes periodically. In volute tongue the pressure fluctuation is small, but in dynamic and static coupling interface which is large. With different flow rate, the pressure fluctuation is also different, the greater the flow rate, the more serious the pressure fluctuation. The main frequency for pressure fluctuation appears in low frequency region, in high frequency region the pressure fluctuation is not obvious. In inlet and outlet the pressure fluctuation is small, less than 1 time of rotation frequency. In impeller blade region the pressure fluctuation is biggish, and mainly to rotation frequency and blade passing frequency, the pressure fluctuation of suction surface is greater than that of pressure surface.

Acknowledgments

The authors gratefully acknowledgement the support of Natural Science Foundation of China (Grant No.51169010) and National Sci-tech Support Plan of China (Grant No. 2012BAA08B05)

Nomenclature

D_2	Impeller inlet diameter[mm]	D_1	Impeller outlet diameter [mm]
b_2	Impeller inlet width[mm]	β_2	Impeller inlet installing angle [°]
$\beta 1$	Impeller outlet installing angle [°]	L	Guide vane length[mm]
S	Impeller thickness [mm]	β_4	Guide vane outlet angle[°]
β_3	Guide vane inlet angle [°]	t	Flow time[s]
Z_1	Impeller vane number	f	Frequency [Hz]
Z_2	Impeller vane number	T	Cycle
H	Head[m]	η	Efficiency[%]

References

[1] Shahram Derakhshan, Ahmad Nourbakhsh,2008,“Theoretical, numerical and experimental investigation of centrifugal pumps in reverse operation,” Experimental Thermal and Fluid Science, Vol.32, No.8, pp.1620-1627.

[2] Yang JunHu, YuanYaFei and Jiang YunGuo,2010,“Performance predictions of reversed centrifugal pumps working as energy recovery turbines,” Journal of Lanzhou University of Technology, Vol.36, No.1, pp.54-56.

[3] J Ferna′ndez, E BlancoJ and Parrondo, 2010,“Performance of a centrifugal pump running in inverse mode,” Journal of power and energy, Vol.18, No. 4,pp. 265-271.

[4] Yang Sunsheng,Kong Fanyu and Shao Fei, 2012,“Numerical calculation and experiment of hydraulic turbine,” Journal of Jiangsu university(Natural Science Edition), Vol.33, No. 3,pp.165-169.

[5] Pradeep Bansal, Nick Marshall, 2010,“Feasibility of hydraulic power from waste energy in bio-gas scrubbing process,” Applied Energy , Vol.87 No.3,pp.1048-1053.

[6] Ying Ma, Eric Kadaj and Kevin Terrasi, 2010,“Flow Factor Prediction of Centrifugal Hydraulic Turbine for Sea Water Reverse Osmosis (SWRO),” International Journal of Fluid Machinery and Systems, Vol.3,No.4, pp.369-378

[7] Tan Minggao,WangYong and Liu Houlin, 2012,“Effects of number of blades on flow induced vibration and noise of centrifugal pumps,” Journal of Drainage and Irrigation Machinery Engineering, Vol.30, No.3,pp.131-135.

[8] Wang Yong,Liu Houlin and Liu Dongxi, 2013,“Effects of vane wrap angle on flow induced vibration and noise of centrifugal pumps,” Transactions of the CSAE,Vol.29, No. 1,pp. 72-77.

[9] Fernandez, J., Blanco, E., 2004,“Performance of a centrifugal pump running in inverse mode,” Proceedings of the Institution of Mechanical Engineers, Vol.218, No. 4,pp. 265-271.

[10]Majidi Kitano,2005,“Numerical Study of Unsteady Flow in a Centrifugal Pump,” Journal of Turbo machinery, Vol.127, No. 2,pp.363-371.

[11] Parrondo-Gayo, Jorge L., González-Pérez and José, 2002,“Fernández-Francos, Joaquín. The effect of the operating point on the pressure fluctuations at the blade passage frequency in the volute of a centrifugal pump,” Journal of Fluids Engineering, Transactions of the ASME, , Vol.124, No.3,pp. 784-790.

[12]Dong, R., Chu, S., Katz, J., 1997,“Effect of modification to tongue and impeller geometry on unsteady flow, pressure fluctuations, and noise in a centrifugal pump,” Journal of Turbo machinery, Transactions of the ASME, Vol.119, No.3,pp. 506-515.

[13] Peter Kerschberger, Arno Gehrer, 2010,“Performance Optimization of High Specific Speed Pump-Turbines by Means of Numerical Flow Simulation (CFD) and Model Testing,” International Journal of Fluid Machinery and Systems, Vol.3, No.4, pp. 352-359

[14]Yang SunSheng, Kong FanYu, Zhang XinPeng, 2012,“Simulation and analysis of unsteady pressure fluctuation in hydraulic turbine,” Transactions of the CSAE, Vol. 28, No.7, pp.67-72.

[15]Zhu Rong Sheng, Hu ZiQiang and Fu Qiang, 2010, “Numerical simulation of pressure fluctuation in double-blade pumps,” Transactions of the CSAE, Vol.26, No.6, pp. l29-134.

[16] Li Yi-bin, Li Ren-nian and Wang Xiu-yong,2013,“The Numerical Simulation of Unsteady Flow in a Mixed Flow Pump Guide vane, " International Journal of Fluid Machinery and Systems, Vol.6, No.4, pp.200-205.

[17]Wang FuJun, Zhang Ling, Li YaoJun, 2008,“Some key Issues of unsteady turbulent numerical simulation in axial-flow pump,” Chinese Journal of Mechanical Engineering, Vol. 44, No. 8, pp.73-77.